AIAA Aviation Forum and ASCEND co-located Conference Proceedings
29 July - 2 August 2024, Las Vegas, Nevada
AIAA AVIATION FORUM AND ASCEND 2024
10.2514/6.2024-4519

Towards the Design of a Bleed-Air Actuator for Single Surface Parafoils

Donald J. Ward *, Andrea L. Vu† and Mark Costello‡
Earthly Dynamics Corporation, Atlanta, GA, 30076, USA

Bleed air actuation using upper surface spoilers is a lightweight, cost-effective control strategy for achieving glide slope modulation in ram air parafoils. The addition of glide slope control to airdrop systems significantly increases the accuracy of terminal guidance strategies and thereby improves the probability of a successful resupply or delivery mission. This work aims to extend the glide slope control capabilities of bleed air spoilers to single surface parafoils. These canopies are lighter weight and lower volume than ram air parafoils of a similar size and offer a more compact, guided aerial delivery solution. However, with significantly differing flow physics from ram-air canopies, single surface parafoils present a novel challenge for the implementation of bleed-air actuators. A 2D CFD model is used to establish a comparison between actuation concepts for control authority and robustness. The bleed-air actuator design problem is abstracted by considering the airdrop concept of operations and the high-level concepts are proposed for each critical function. The most relevant concepts are flight tested in unpowered flight and video footage is used to evaluate opening and sealing behavior. A counter-weighted design is found to fulfill the design requirements of reliable sealing and venting of bleed-air, at the cost of increasing system weight.

Nomenclature

BAA	=	bleed-air actuator
c	=	chord, m
C_d	=	drag coefficient
C_l	=	lift coefficient
C_p	=	pressure coefficient
L/D	=	glide ratio, n.d.
LE	=	leading edge
LEI	=	leading edge inflated
TE	=	trailing edge
V_∞	=	freestream velocity, m/s
α	=	angle of attack, deg

I. Introduction

Aerial delivery and recovery missions often rely heavily on impact location accuracy as a measure for success. In ballistic or unguided systems, the impact location is determined by the initial conditions of the deployment and atmospheric wind conditions during the descent. Due to the variable nature of these factors, ballistics systems are susceptible to a degree of uncertainty in their impact location. Guided airdrop systems, on the other hand, offer a tremendous accuracy advantage over ballistic parachutes by enabling active steering to a target point. Ram-air parafoils are examples of such a system. Steering of ram air parafoils is achieved by asymmetric deflection of the trailing edge while airspeed can be reduced with symmetric trailing edge deflection. Because this control scheme does not offer direct glide slope control, autonomously guided systems perform a series of S-turns to dump altitude as the impact location is approached [1]. The duration of this maneuver is determined by the system's estimated glide ratio and wind velocity

*Research Engineer, Student Member AIAA.
†Engineer
‡Chief Executive Officer, Associate Fellow AIAA

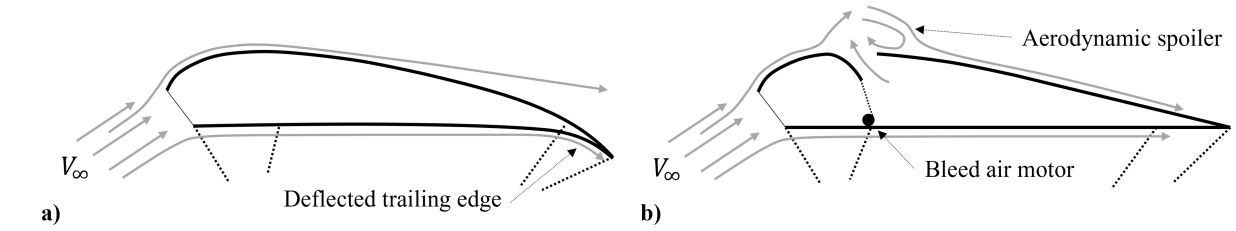

Fig. 1 Ram-air control techniques: a) conventional, TE deflection and b) bleed-air actuation

estimate [2]. Because the local wind velocity is calculated at a higher altitude, variations in the wind field, especially as the guided system approaches the ground, can still induce significant offsets in trailing edge controlled systems.

Upper surface bleed air spoilers have emerged as a highly effective, direct glide slope control strategy for ram air canopies. Bleed-air actuation is achieved in ram-air canopies by adding vents in the upper skin which are pulled open via a control line [3–5]. As the opening increases in size, the high pressure ram air is vented over the upper surface, spoiling the lift of the canopy. As the control input is diminished, the pressure differential across sealing flap closes the vent and canopy glide performance is restored. With symmetric actuation across the span of the canopy bleed air actuation reduces the glide slope whereas asymmetric actuation influences turn rate. This control method has been successfully fielded by Scheuermann et al. and León et al. in a variety of autonomous airdrop systems, requiring less actuator mass and energy than comparable trailing edge systems [5, 6].

To date, ram-air canopies are the only textile-based parafoils to implement bleed-air spoilers for direct glide slope control. However, as the aerial delivery and recovery mission space evolves, there is an emerging need for compact, lightweight, and cost-effective parafoils. Single surface parafoils are a compelling solution for this need, offering similar steering and glide performance as ram air canopies with less canopy material and simpler construction. Examples of these canopies are shown in Figure 2. Rather than having an open leading edge single surface parafoils have a closed leading edge, commonly reinforced with stiffening elements or inflated spars. The lifting surface is formed from a single sheet of fabric and therefore lacks a pressurized internal cavity. This pressurized air is a driving force for bleed air spoilers in ram air canopies, responsible for sourcing the bleed air and closing the sealing flap when unactuated. By lacking the internal ram air pressure, single surface parafoil construction differs significantly from ram air canopies and presents a novel use case for bleed air spoilers.

II. Prior Work

Prior work has investigated the possibility of implementing bleed-air spoilers on single-surface parafoils. Ward et al. conducted flight testing of a bleed-air vents on a small-scale, paragliding-style canopy. Vents were fabricated in a

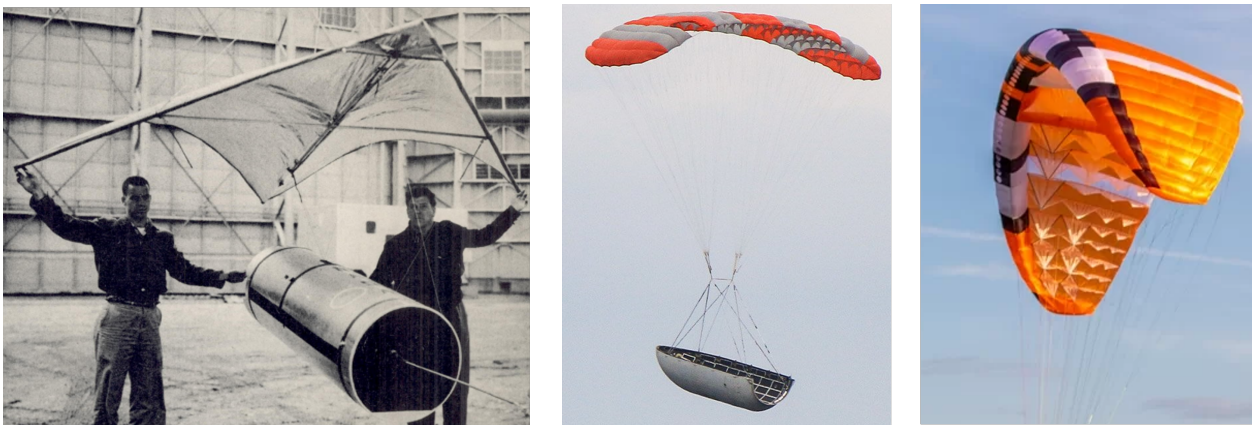

Fig. 2 Single surface canopies: Rogallo parawing for booster recovery [7] (left), Falcon 9 fairing recovery parafoil [8](middle) , and recreational paraglider [9](right)

chordwise and spanwise grid and opened in parametric configurations prior to flight. Ward demonstrated that bleed-air is indeed a viable mechanism for achieving lateral and longitudinal control [10]. Uncontrolled openings were tested at 0.1c, 0.3c, 0.5c, and 0.7c across 88% of the canopy span. Results showed that openings at 0.1c were the most effective, reducing the glide slope by 58% and inducing turn rates of 38 deg/sec. Additionally, the glide slope and turn rate responses were shown to be largely linear with the number of vents opened. This work highlighted that locating the BAAs near the LE is critical for achieving control response. However, this prior investigation was performed with static openings, shown in Figure 3a, meaning that the bleed-air vents did not have sealing capability. This current work aims to develop a controllable BAA, as conceptualized in Figure 3b, that can produce controllable glide slope changes by opening and closing.

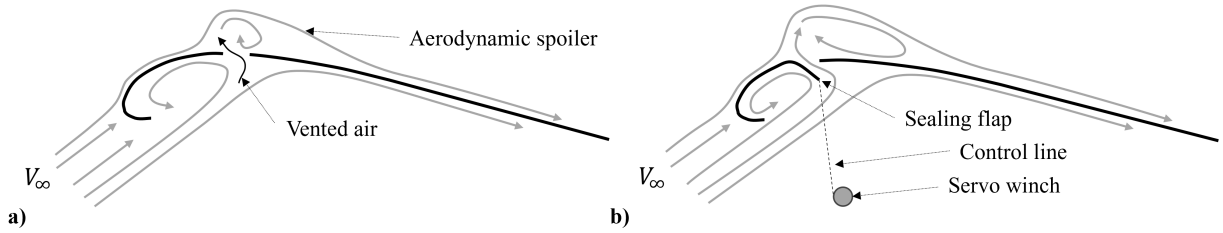

Fig. 3 a) Uncontrolled bleed-air vents examined by [11] b) Conceptual, controllable BAA

In the development of BAAs for ram-air canopies, the knowledge of the nominal and induced flow field was useful in estimating and understanding the spoiling and sealing effect of various vent designs. Gavrilovksi found that the direction of the vented, bleed-air to the upper surface does impact the spoiling effect, where LE-facing vents were shown to produce more control response than LE-facing vents [4]. A CFD and wind tunnel analysis by Bergeron investigated the flow physics of the BAAs in ram-air canopies. A 2D CFD analysis was compared with pressure measurements and smoke injected flow behavior [12]. The BAA was shown to produce a large region of separated flow between the BAA and the TE when opened, and restore attached flow when unactuated. Later implementation of the BAA on a 9.2m^2 ram-air system required elastic bands to support the control line weight and drag and faciliate sealing when unactuated [13]. It is assumed that similar complications may exist for developing BAAs for single surface canopies. However, because the single surface construction differs significantly from ram-air canopies, ram-air flow physics may not be applicable for designing single surface BAAs.

There is little literature investigating the flow field surrounding single surface parafoils. However, prior work has investigated airfoils with similar geometry such as Rogallo-style parawings [14] and LEI kites. Parawings are constructed with a single skin supported by rigid elements or inflatable spars along the LE to form two partial conic sections. These wings glide with high angle of attack (25° - 41°), relative to conventional parafoils, and attain longitudinal control by modulating canopy trim angle. Using a rigid surrogate, Fournier [15] measured the pressure distribution on the lower and upper surface of a parawing in a wind tunnel. It was demonstrated that like a ram-air canopy, the pressure differential is greatest near the LE and tapers off towards the trailing edge. However, unlike ram-air canopies, stagnation pressure is not achieved on the lower surface, which has an average C_p of approximately 0.6 for the majority of the chord. While the geometry of parawings differs from from single surface parafoils, this result could explain the emphasis of placing BAAs near the LE for attaining meaningful glide slope control.

Finally, academic interest in LEI kits has increased as these canopies pose promising benefits for airborne wind energy harvesting [16]. As result, there is literature investigating the flow physics of LEI kites, which have a similar chordwise cross section to single surface parafoils. Folkersma [17] performed 2D CFD analysis of the flow field over an LEI kite with varying camber. This study also found that the lower surface pressure is less than stagnation pressure. In addition, recirculating flow was indicated between the inflated LE and $0.4c$. This behavior is in direct contrast to ram-air flow physics, which are inflated with largely stagnated airflow. Both parawing and LEI investigations indicate that single surface canopies have significantly differing flow physics from ram-air canopies, and therefore merit an individual investigation into BAA design for these canopies.

This work lays the basis for the design of a BAA for single surface canopies. First, a two-dimensional CFD model of the test canopy is analyzed to understand nominal flow physics. The model is then modified with generic BAA designs and evaluated for spoiling and sealing capability. Based of these results and prior work, BAA designs are conceptualized based upon core functionality. Select geometries are prototyped and flight tested. An onboard camera records the state

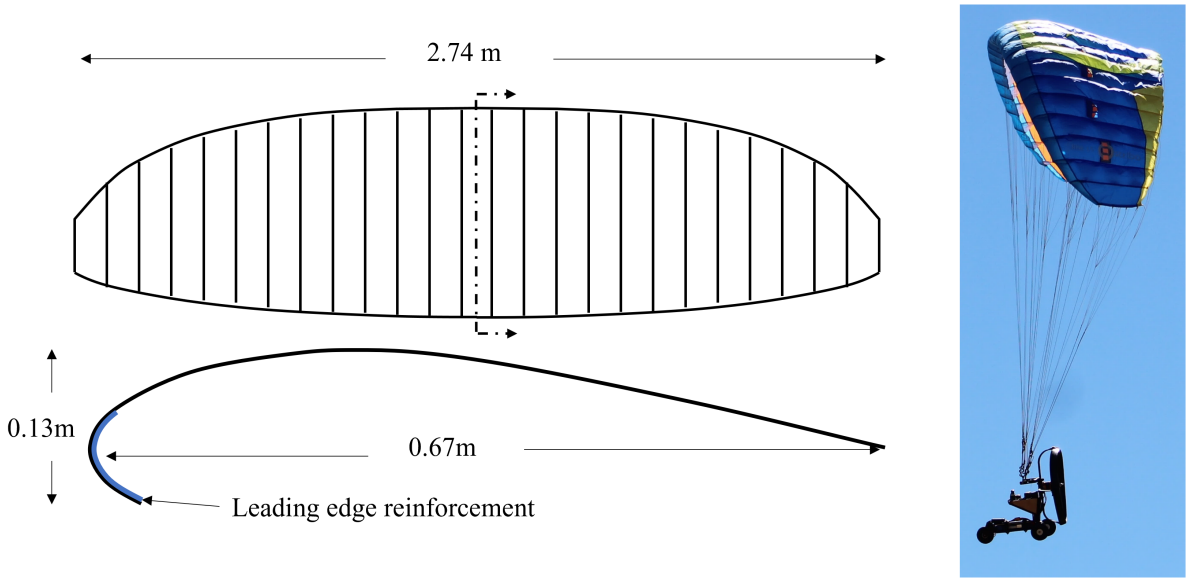

Fig. 4 Dimensions of experimentation canopy (left) and test platform in flight with custom paramotor payload (right)

of the canopy and the BAA designs to evaluate performance.

III. System Description

The canopy and flight vehicle, shown in Figure 4, used for computational analysis and flight test is identical to the system used by Ward [11]. The wing is elliptical in planform and has a cross-section approximated by a NACA 23015 airfoil. The center chord is 0.67m, and the tip chord is 0.22 m. The leading edge is reinforced with plastic stiffening elements sewn between the single skin and the walls of each semi-cell. The canopy has a constructed wingspan of 2.74m and a corresponding area of 1.5m^2. In flight, the projected area is 1.27m^2. The overall weight of the wing, including the riser hardware, is 154g. When flown with the 1.96kg RC paramotor platform, the S-Lite canopy has an approximate glide ratio of 5.0 and a total airspeed of 5.4 m/s. The paramotor has an onboard camera to record the state of the canopy and BAAs in flight.

IV. Computational Analysis

Computation analysis of the single surface, paragliding canopy was performed to characterize the flow field dynamics on the upper and lower surface of the parafoil. The scope of the analysis was limited to 2D, static simulations. While this restriction limits the fidelity of the model, a methodical approach was employed to draw comparisons between the simulated BAA designs and the nominal canopy. The key areas of focus are pressure differential and flow field surrounding the nominal canopy, glide reduction of the BAA with respect to vent opening, and the sensitivity of the sealing performance with response to BAA design.

A. Setup

The geometry of the modeled canopy is identical to geometry previously investigated by [10]. The parafoil shape is approximated with the upper surface and nose of a NACA 23015. The lower surface is cut away to match the size of the lower surface lip of the SLite parafoil. The thickness of the parafoil is 0.15mm. The parafoil is modeled as a rigid material, disregarding the complicated fluid structure interactions that result in billowing of the canopy. This simplification further limits the extension of the CFD analysis to the physical system.

Two, notional BAA designs are considered in the CFD analysis. LE-facing and TE-facing actuators, shown in 5, are located at $0.1c$. Each bleed-air opening is 0.037c in length. The actuator location and size are chosen to represent the values test in[11]. The opening is sealed with a linear flap with the equivalent thickness as the canopy skin. The flap

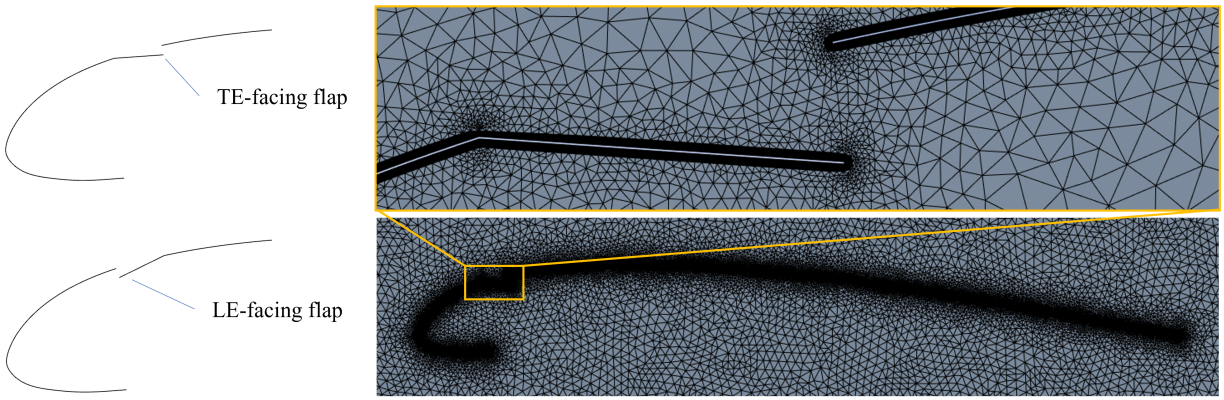

Fig. 5 BAA geometries modeled (left) and computational mesh of the single surface paraglider with notional bleed-air vent with a 5° opening (right)

connection to canopy is modeled as a hinge joint with a sharp interior corner and radius on the upper surface. The sealing flap is identical in length to the bleed-air opening, such that a 0m/s flap opening produces an identical geometry to the nominal, unmodified airfoil. The openings of the BAAs are parametrized by flap angle with respect to the opening.

The computational domain was 15c in length, streamwise, and 10c in the transverse direction. The parafoil was located 5c downstream from the inlet and centered in the transverse direction. An unstructured mesh, shown in 5, was used for the variable geometry of the parafoil. The boundary layer grid on the upper and lower surface is constructed of 30 layers with an initial cell height of 5.2e-6c and a growth rate of 1.1. To maintain consistency between the varying geometries, the upper and lower surface are discretized by 7.46e-04c (0.5mm), resulting in approximately 1400 points on each surface. The resulting mesh, is shown in Figure 5, contains approximately 1.8e6 elements with an average skewness of 0.25 and max skewness of 0.9.

The boundary conditions are informed by the steady flight data collected by Ward [11]. The freestream velocity at the inlet was specified as 5.4 m/s. The Spalart-Allarmas turbulence model is used due to its computational efficiency. Simulations were performed until C_l and C_d were converged or a maximum of 1000 iterations. For TE-facing flap openings greater than 19°, the force coefficients did not meet convergence criteria and instead oscillated by a maximum of 5%. Therefore, the averages of these values were taken from the last 50 iterations. The lack of convergence for these simulations indicate that a transient analysis would provide further information of the flow physics at these vent openings.

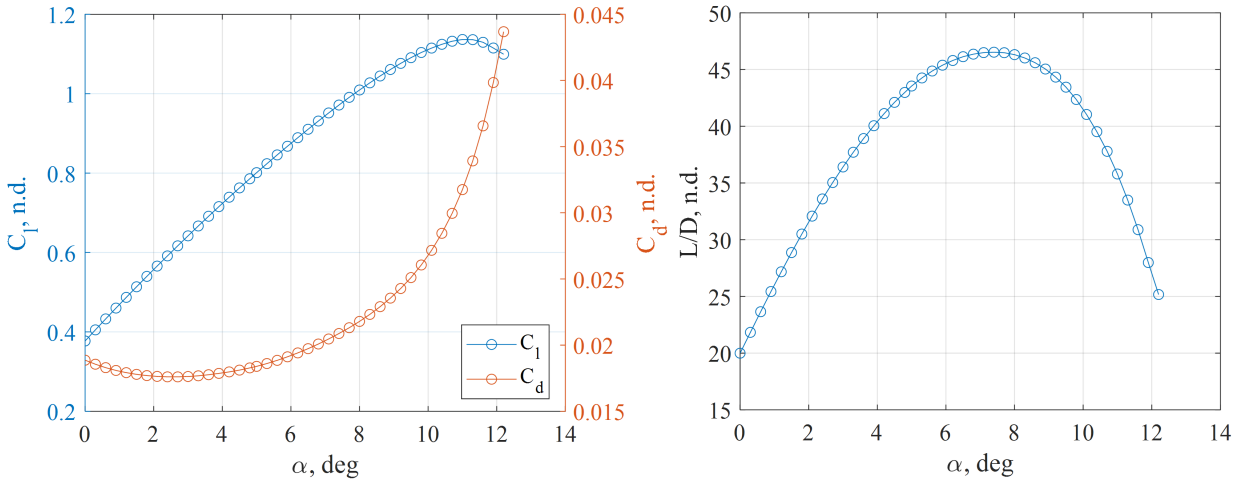

Fig. 6 Force coefficients (left) and glide ratio (right) of 2D single surface parafoil with respect to angle of attack

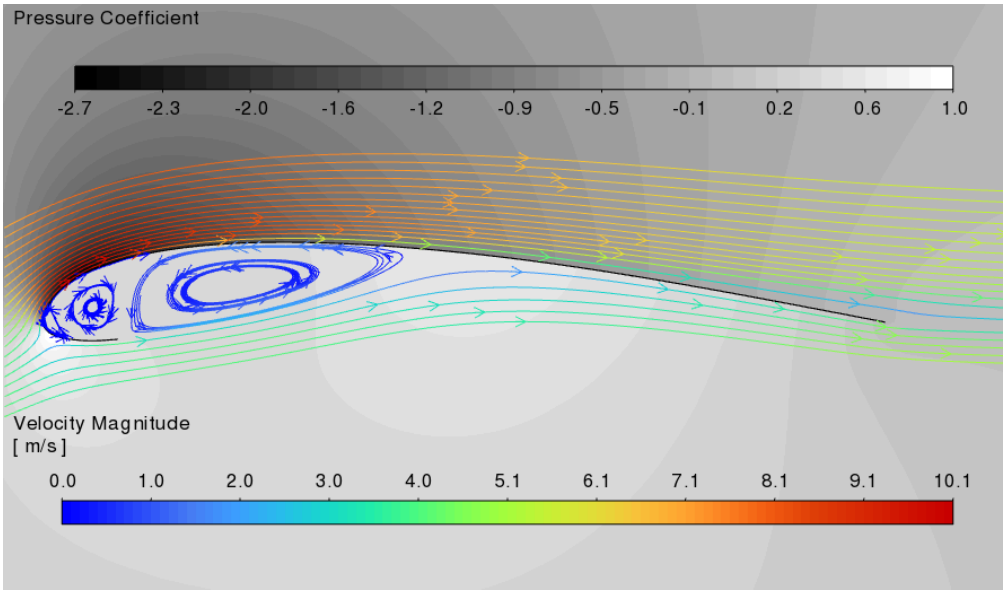

Fig. 7 a) Flow streamlines and pressure coefficient contour of nominal single surface paraglider at α = 7.4°

B. CFD Results and Discussion

The 2D CFD of the baseline, un-modified canopy is first analyzed. Given the rigging geometry, the physical canopy is permitted to pitch relative to the payload. Therefore, instead of picking a single angle of attack to analyze the parafoil, the angle of attack was varied from 0° to 12.2°. Figure 6 shows the variation of the force coefficients and glide ratio. C_l increases with angle of attack until approximately 11.5° whereas C_d increases sharply with angle of attack beyond 3°. The maximum glide ratio of 46.3 was achieved at 7.4°. Prior simulation of this canopy assumed an α = 11.7, but demonstrated a region of separated flow beyond 0.75c. Therefore, the pressure coefficient contour and streamline velocities are shown for α = 7.4° in Figure 7. Airflow remains attached for entirety of the upper surface. Flow recirculates on the lower surface, near the leading edge. In addition, the pressure coefficient on the lower surface indicates pressure is above stagnation pressure. These results are in agreement with streamer behavior recorded while flight testing the SLite canopy [10]. The flow field is comparable to the CFD investigations of the LEI kites as well as the pressure on on the lower surface of parawings.

C. Bleed-air vent modeling

TE-facing and LE-facing flaps were investigated. The flow effects of the TE and LE flap at 11° opening are compared in Figure 8. At this opening size for LE-facing flap, the pressure distribution about the canopy is largely unchanged from the nominal case, with the exception of reduction in pressure on the under surface near the recirculation zone. However, the velocity of upper surface flow is reduced and flow begins to separate from the upper surface at 0.65c. In contrast, the aerodynamic spoiler produced by the TE-facing flap is much more pronounced. Upon meeting the forward flowing bleed-air, airflow is separated from the upper surface for the rest of the airfoil. Accordingly, the pressure differential across the canopy is reduced by more than 50% near the leading edge. At this flap opening angle, the glide ratio of LE-actuated airfoil is 28.5:1, while the glide ratio of the TE-actuated airfoil is 15.7:1. Qualitatively, the pronounced difference in the glide slope reduction between the flap directions aligns with the results from [4].

To gain further understanding of the glide ratio response, the opening angle was varied from 1° to 43°, with greater granularity from 1° to 7°. The glide ratio effects of the TE and LE flaps are compared in Figure 9. Both flap configurations achieve similar minimum glide ratios of approximately 15:1. However, the TE-flap provides a much greater reduction in glide slope with flap opening angle and saturates in response between 5° and 10°. These results are in agreement with prior flight testing comparison of LE and TE bleed air vents performed by [4] which found the that TE vents were more effective bleed-air actuators in ram-air canopies.

Finally, the implications of flap direction on sealing capability is considered. It is expected that opening a bleed-air actuator will reduce the pressure differential across the sealing flap and therby reduce the aerodynamic force that is responsible for sealing the BAA when unactuated. The local pressure differential across the sealing flap is considered

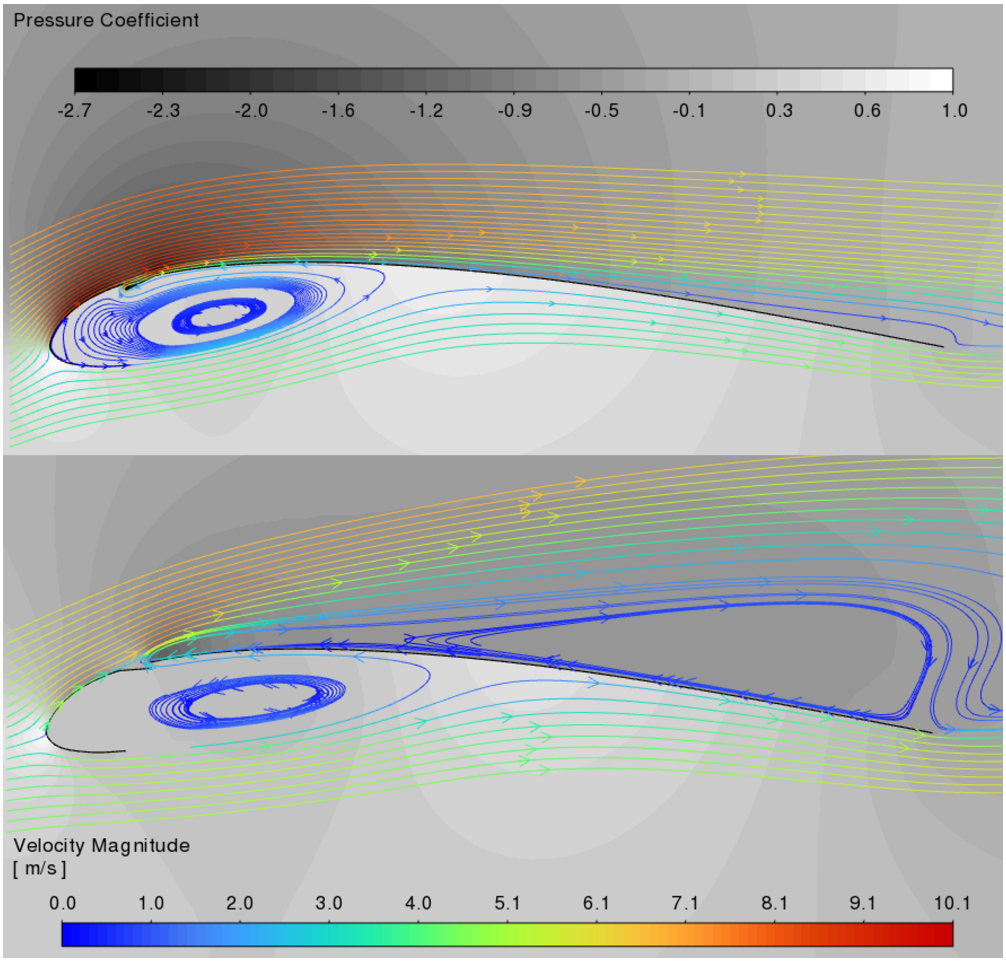

Fig. 8 Flow field comparison of LE-facing (top) and TE-facing (bottom) flaps open at 11°

for both LE and TE-facing flaps at 11° opening. The LE flap has an average pressure differential of 35Pa while the TE flap has an average of 13Pa. This model is not expected to match real-world static pressures of BAAs, but the 3x difference between the actuator configurations does indicate that the LE-flap may seal more readily than the TE-flap when perturbed from the sealed position.

V. BAA Design

The task of design of bleed-air actuator for single surface parafoils is abstracted by considering constraints, objectives, and variables. The actuator should be designed with airdrop mission in mind but is restricted by the test vehicle and methods that are currently used to evaluate BAAs for single surface parafoils at small scale.

A. Constraints and Objectives

The primary design constraint for the BAA is twofold: it must effectively control glide slope by venting air when activated and must seal effectively when deactivated to restore canopy performance. The latter is crucial for two reason. First, implementing BAAs with direct glide slope control at the cost of dramatically reducing the nominal glide limits utility of BAAs for longer range missions. Secondly, reducing the maximum glide ratio of system limits the range of glide slope control authority. The extent of control authority provide by venting air is less critical as increasing the number of actuators across the canopy can compensate for any individual actuator's performance limitations in reducing glide slope. Another critical constraint is that the actuator design must function effectively at the small scale of the current test platform, which is designed for Group 1 UAVs. This scale allows for cost-efficient, low-risk, rapid

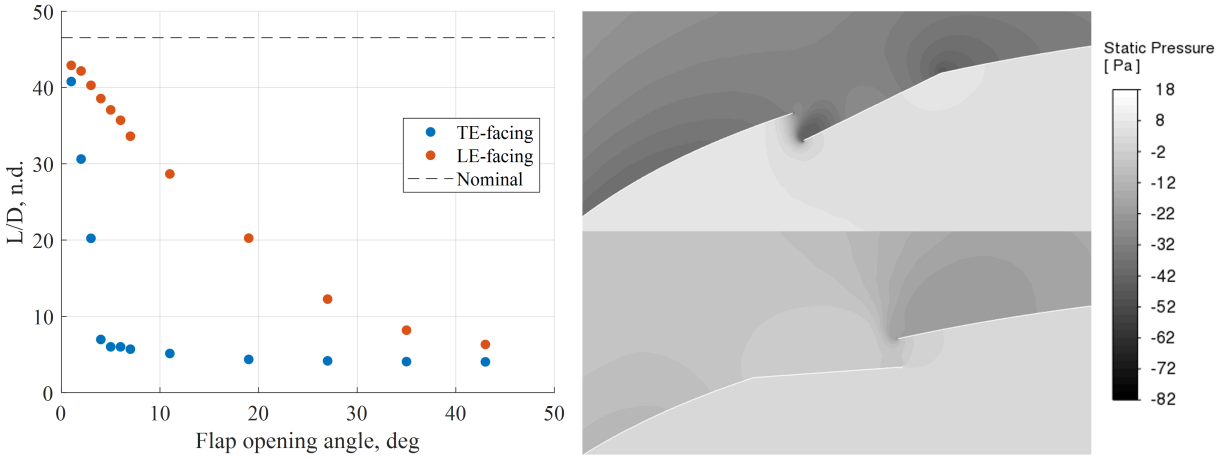

Fig. 9 Parametric sweep of flap opening angle and glide ratio effect (left) and comparison of static pressure distributions for a11° flap opening(right)

development and evaluation of control and actuation methodologies, and meets FAA regulatory requirements. However, this constrain precludes the use of large or heavy power sources that do not scale to this small vehicle. Additionally, some COTS materials, such as control lines, may not scale to the small actuation forces, and therefore cause more drag than the optimally-sized control line. The BAA design for this effort must be robust to this non-ideality.

The design objectives for the bleed-air actuator are informed by the airdrop application. In airdrop and or emergency recovery scenarios, the packability of decelerators and control systems is crucial. This objective encompasses both the compactness of the decelerator's overall pack volume and the flexibility of integrated components within the canopy required for bleed-air control. It is essential to minimize the size and stiffness of materials that increase the overall pack volume and impede or potential cause damage during packing and deployment.

Another objective is that the materials and forces applied to the canopy to achieve BAA control should produce minimal canopy deformation. Canopy deformation will disrupt the flow field, obscure the intended effects of BAA, and hinder the ability to evaluate BAA designs. Additionally, if actuation power is causing deformation, this indicates that the actuator is not energy efficient, and requires higher loads than necessary to actuate the spoiler. This increase in actuation loads, especially at larger vehicle scales, will require large actuators and energy sources, compounding the size and weight penalty. Finally, the introduction of control lines for actuators adds drag and can degrade the canopy's glide performance. Actuator designs that minimize additional drag from control lines are preferred to maintain optimal canopy performance during deployment and operation.

In summary, the bleed-air actuator must meet functional requirements such as providing direct glide slope control and ensuring the aerodynamic spoiler opens and seals as needed. Development is constrained by the small-scale test platform and regulatory considerations, emphasizing usability and operational efficiency in flight testing scenarios. The design objectives are driven the airdrop and aerial recovery missions, which favor small, lightweight, and energy efficient systems.

B. Design Variables

A notional BAA with a vent opening, sealing flap, and control line is described. Key design variables are identified that correlate with the stated design constrain and objectives. Multiple concepts are proposed for each design variable and grouped to synthesize complete designs.

1. Actuator Geometry

The notional BAA is shown in Figure 10. For comparison, the actuation concepts design are implemented on identical sealing flap geometry, which is sized to haved similar opening area as the vents evaluated in [11]. The total opening area of the bleed air actuator is 21.5cm^2 or 0.17% of the canopy's projected area. Chordwise reinforcements provide strength and prevent the sealing flap from protruding through the opening when sealed. The sealing flap is larger

than the vent, providing a margin of 8mm around the perimeter of the opening. The flap is secured to the canopy with ripstop tape at the leading edge side of the opening. The openings are reinforced with ripstop tape around the perimeter. The control line is attached to the tip of the flap and the servo winch on the payload. The total weight of the 40D nylon sealing flap is 1.4e-3N. The required length of the control line is nominally 150cm in length and weighs 3.2e-3N.

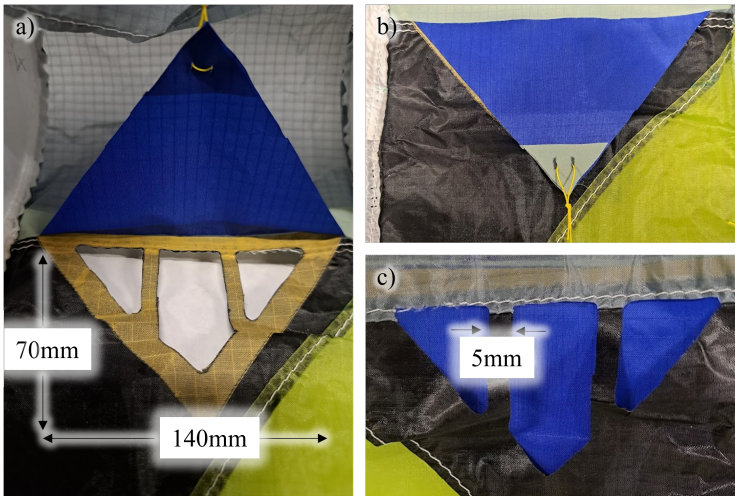

Fig. 10 Generic sealing flap for testing actuator designs: Bleed air opening (a) and sealing flap (b) from underside of canopy and sealed vent from top surface (c).

2. Opening direction

The vented flow direction is assumed to impact sealing capability and overall control authority based upon the 2D CFD analysis as well as prior work investigating BAAs for ram-air canopies. Small deflections in flap from control weight or other disturbances could interact with the local airflow, peeling the sealing flap away from the canopy. Flap direction may also determine the direction of air vented to the upper surface and therefore the effectiveness of the aerodynamic spoiler. Both LE-facing and TE-facing BAAs are within the scope for this design effort.

3. Control method

The use of a servo winch to contol the bleed-air actuator bounds the design space to solutions that are controllable with control line, akin to trailing edge and bleed-air spoilers in ram-air parafoils. Possible concepts that address the core functions or opening and sealing are identified in Figure 11. The concepts are also categorized by active (using the servo winch to achieve the function) or passive. A single control line can only impart forces on the sealing flap via tension, is thereby limited to only sealing (through the use of a pulley) or opening the vent, not both functions simultaneously. Therefore, passive techniques may be used to accomplish the opposing task. Active opening methods are first considered, as these require the least additional components to the canopy and are the current fielded method for BAA in ram-air canopies. The simplest passive option to seal the vent is relying on the pressure differential to reseal the flap when control line is payed out. An alternative is using an antagonistic spring element, such as a elastic band, to support the flap and control line weight and facilitate sealing. The length and attachment location of the elastic element is tunable to find optimal and reduce canopy deformations.

In contrast, an elastic element could be used to open the flap while the control line, via a pulley, closes it. Finally, the weight of the sealing flap could act as a sealing feature, supplying sufficient force to oppose the pressure differential and open the flap when control line is payed out. This method likely incurs a weight penalty to the BAA, as the pressure distribution at the 0.1c chord location indicated by CFD is sufficient to support a seal flap. Weight may be located as far from flap-canopy joint as possible to reduce amount of weight required. However, the counterweight concept is likely to impose minimal canopy deformation . The active closing techniques provide the distinct advantage of ensuring the BAAs is closed with a determined control line length, but with the requirement of a pulley or other redirection element.

The active and passive control methods are combined, as shown in Figure 12, to conceptualize fully-functional

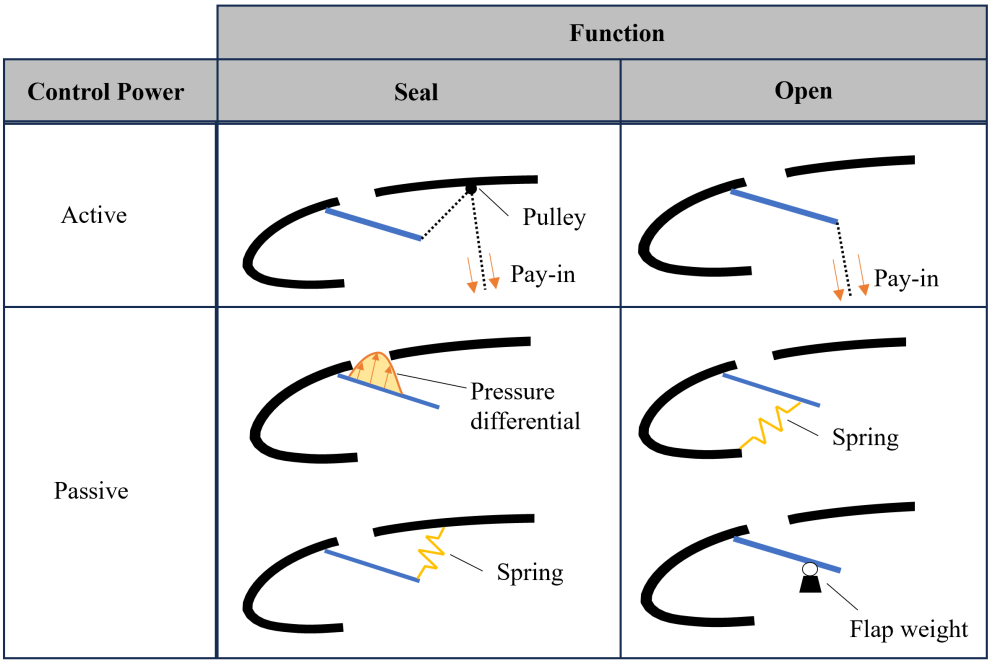

Fig. 11 Morphological chart of the sealing and opening methods

BAAs. A control line can only impart forces on the sealing flap via tension and is thereby limited to only sealing (through the use of a pulley) or opening the vent, not both functions simultaneously. Therefore, passive techniques may be used to accomplish the opposing task. Another option is the bi-directional, active control option. In this concept, the servo winch utilizes a continuous line to control both sealing and opening of the flap with the rotation of the spool. This method requires twice the amount of control line per BAA, increasing system drag. Additionally, the kinematics of arc path of flap-control line attachment point is not compatible the relative length changes between the winch, flap, and pulley. However, this could be mitigated by optimizing the geometry for minimal deformation in the canopy and sealing flap.

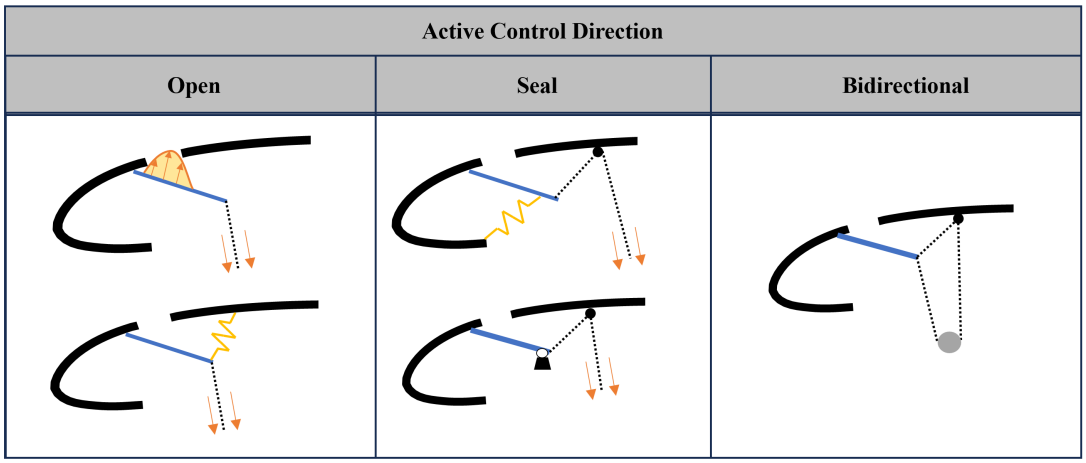

Fig. 12 Synthesis of conceptual bleed-air actuator designs from individual sealing and opening methods.

VI. Flight testing

A. Method

The RC paramotor is used to perform, unpowered glide tests of the BAA designs. An onboard camera records the canopy for deformation and the state of the BAAs. Streamers are added in the vicinity of the vents for the visualizing flow effects. Flights are long enough to assess steady state behavior of the BAAs and obtain video footage. This method is used as opposed to collecting steady flight data given the large design space and the amount of flight data required to build confidence in the control response. Short, unpowered flights allows for rapid turn time and design iteration.

B. Preliminary results

The simplest flap design concepts were tested first. LE and TE-facing flaps were fabricated on the SLite canopy. To investigate the complications of the flap weight, control line weight, and drag on the sealing performance, these aspects were tested sequentially. These flaps were first tested without control line, as shown in Figure 13a. Without control line, both flap directions were found to seal without issue. Additionally, the LE-flaps are shown to adhere to the underside of the canopy in the absence of a bleed-air vent and a pressure differential. However, when control lines are added and configured to permit opening without excess slack, both TE and LE-flaps remain open. The change in sealing behavior with addition of control flaps indicates that the control line weight and/or drag are a critical factor for this vent design. To mitigate this, sheaveless, pulley-like elements were integrated into the canopy to support line drag. Three versions were tested as shown in Figure 13c. None of the pulley concepts were successful in achieving flap sealing, but the LE-facing flap with the forward pulley had the smallest opening.

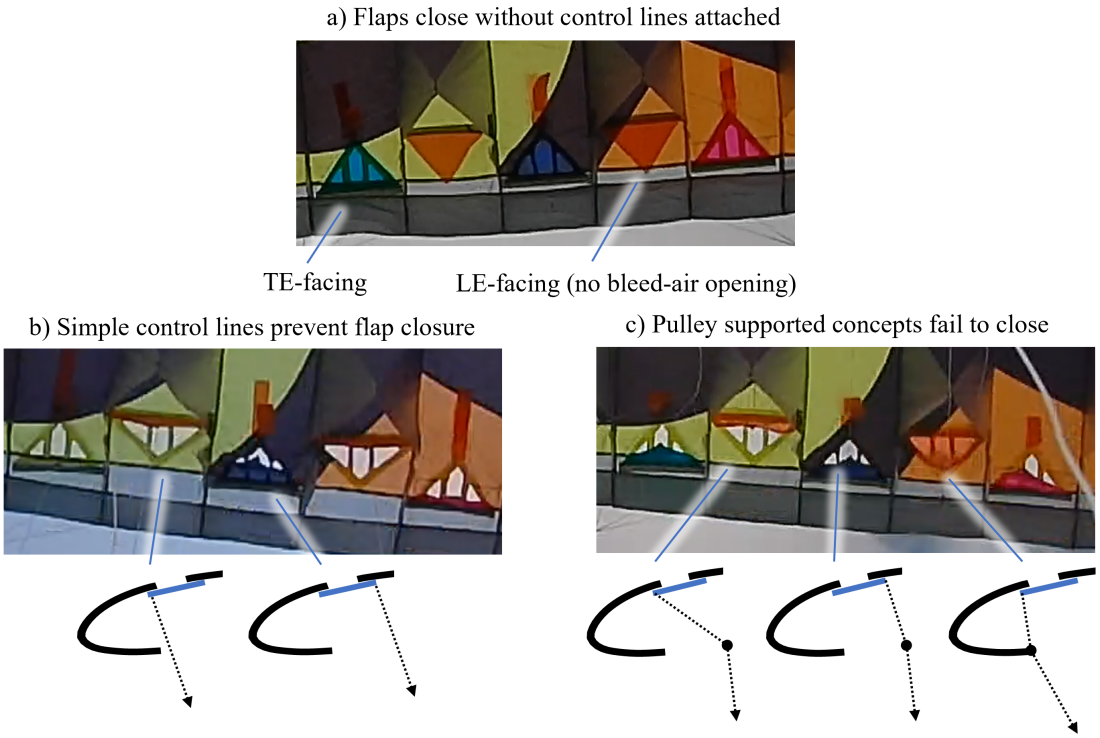

Fig. 13 Sequential testing of the active-open flap concepts

The active-opening configuration of the elastic actuator design were prototyped and tested. Elastic bands were attached to both sides on the semi-cell, aft of the TE-facing flap. The control line was attached to the center of the band, and slack was added between the band and the sealing flap. The slack length of the control line and elastic band was tuned to require 0.8N to fully open the vent. Upon glide testing, the sealing flap was found to close (Figure 14), adequately supporting control line weight. However, upon opening the flap, large deformation in the leading edge was noted in the canopy. The geometry of the elastic band can be tuned to reduce control force but the cross section of the

elastic band is the smallest that is COTS available. The length of the band would need to be increased to reduce canopy deformation.

Finally, the counterweight concept was prototyped. Control line was routed through the pulley and attached to the flap. The counterweight was stitched to the apex of the flap. During glide testing, the weight was incrementally increased until the flap opened when control line was payed out. The minimum weight required to open the sealing flap was 3.1e-3N. The performance of the counterweight concept is shown in Figure 14. With control line payed-in, the sealing flap is closed. When payed out, the sealing flap is completely open. Operation of the counterweight concept induces minimal canopy deformation. If this method is employed to actuate the single surface canopy to achieve similar control authority in [11], the weight of the canopy would increase by 2-3%.

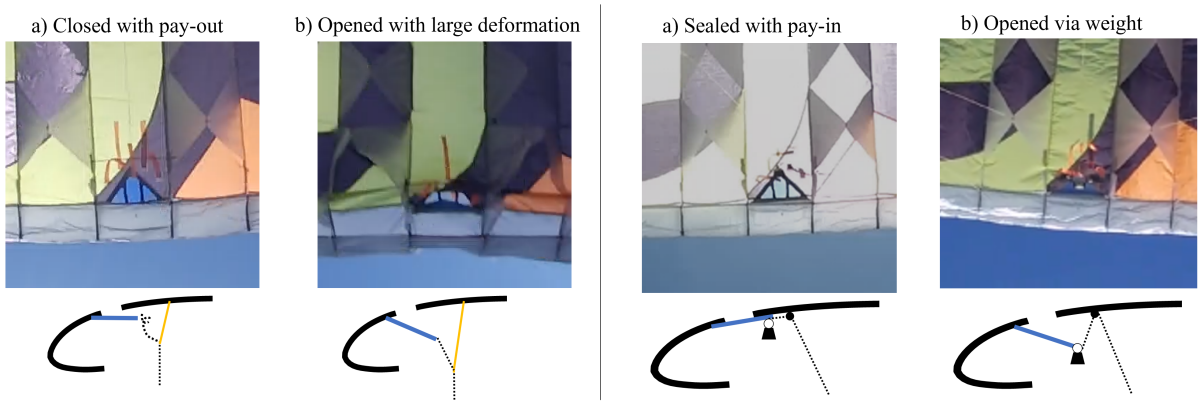

Fig. 14 Glide testing of prototype actuator designs: active-open, elastic (left) and active-closed, counterweight (right) concepts

VII. Conclusion

The flow physics of single surface paragliding canopies present unique challenges for developing BAAs aimed at achieving turn rate and glide slope control. Previous research has shown the feasibility of using bleed-air for these purposes, setting the stage for the development of in-flight controllable BAAs. This work used two-dimensional CFD analysis to find that TE-facing flaps may offer superior aerodynamic spoiler and control authority compared to LE-facing flaps, despite potential complications in sealing due to minimal pressure differentials. This finding indicates that TE-flaps may be more effective for BAAs in single surface canopies. The design problem for BAAs was approached by brainstorming various sealing and opening concepts, leading to the identification and prototyping of several BAA designs. Glide testing of select prototypes evaluated their potential. A counter-weighted design was found to provide the desired opening and sealing behavior, at the penalty of increasing the canopy weight by 2-3% when fully implemented. Future efforts will focus on refining sealing capabilities and further testing these prototypes to develop a fully-actuated single surface canopy.

References

[1] Petry, G., Behr, R., and Tscharntke, L., "The parafoil technology demonstration (PTD) project: Lessons learned and future visions," *15th Aerodynamic Decelerator Systems Technology Conference*, 1999. https://doi.org/10.2514/6.1999-1755.

[2] Scheuermann, E. J., Ward, M., Cacan, M. R., and Costello, M., "Combined lateral and longitudinal control of parafoils using upper-surface canopy spoilers," *Journal of Guidance, Control, and Dynamics*, Vol. 38, No. 11, 2015, pp. 2122–2131. https://doi.org/10.2514/1.G000892.

[3] Gavrilovski, A., Ward, M., and Costello, M., "Parafoil glide slope control using canopy spoilers," *21st AIAA Aerodynamic Decelerator Systems Technology Conference and Seminar*, 2011, pp. 1–12. https://doi.org/10.2514/6.2011-2517.

[4] Gavrilovski, A., Ward, M., and Costello, M., "Parafoil control authority with upper-surface canopy spoilers," *Journal of Aircraft*, Vol. 49, No. 5, 2012, pp. 1391–1397. https://doi.org/10.2514/1.C031685.

[5] Scheuermann, E. J., Ward, M., Costello, M., Bergeron, K., and Noetscher, G., "Bleed air control: Towards the complete in-canopy system for autonomous aerial delivery," *24th AIAA Aerodynamic Decelerator Systems Technology Conference*, 2017, pp. 1–12. https://doi.org/10.2514/6.2017-3883.

[6] León, B., Wachlin, J., Ward, M., and Costello, M., "Experimental Flight Tests of an In-Canopy System for Autonomous Aerial Delivery," *26th Aerodynamics Decelerator Systems Conference*, American Institute of Aeronautics and Astronautics Inc, AIAA, 2022, pp. 1–14. https://doi.org/10.2514/6.2022-2717.

[7] Rogallo, F. M., "Paraglider Recovery Systems," Tech. Rep. N-62-12819, National Aeronautics and Space Administration, Langley Station, Hampton, Va, 5 1962.

[8] SpaceX, "Falcon 9 fairing halves deployed their parafoils," Twitter, ???? URL https://x.com/SpaceX/status/1002268835175518208/photo/1, accessed: 01 July 2024.

[9] "Dudek V-King," Webpage, ???? URL https://dudek.eu/en/produkt/v-king/, accessed: 01 July 2024.

[10] Ward, D. J., Vu, A. L., Ward, M., and Costello, M., "Bleed-Air Control of a Single Surface Parafoil Canopy," American Institute of Aeronautics and Astronautics Inc, AIAA, 2022. https://doi.org/10.2514/6.2022-2716.

[11] Ward, D. J., Vu, A. L., and Costello, M., "Control Authority of a Single-Surface Parafoil with Bleed-Air Spoilers," *Journal of Aircraft*, Vol. 0, No. 0, 0, pp. 1–7. https://doi.org/10.2514/1.C037791, URL https://doi.org/10.2514/1.C037791.

[12] Bergeron, K., Ward, M., and Costello, M., "Aerodynamic effects of parafoil upper surface bleed air actuation," *AIAA Atmospheric Flight Mechanics Conference 2012*, , No. August, 2012. https://doi.org/10.2514/6.2012-4737.

[13] Bergeron, K., Ward, M., Costello, M., and Tavan, S., "AccuGlide 100 and Bleed-Air Actuator Airdrop Testing," *AIAA Aerodynamic Decelerator Systems (ADS) Conference*, 2013. https://doi.org/10.2514/6.2013-1378.

[14] Rogallo, F. M., Sleeman, W. C. J., and Croom, D. R. C., "Resume of Recent Parawing Research," Tech. Rep. TMX-56747, National Aeronautics and Space Administration, Langley Station, Hampton, Va, 7 1965.

[15] Fournier, P. G., and Bell, B. A., "Low subsonic pressure distributions on three rigid wings simulating paragliders with varied canopy curvature and leading-edge sweep," Tech. Rep. D-983, National Aeronautics and Space Administration, Langley Air Force Base, Va, 10 1961.

[16] Ahrens, U., Diehl, M., and Schmehl, R., *Airborne Wind Energy*, Green Energy and Technology, Springer, 2013.

[17] Folkersma, M., Schmehl, R., and Viré, A., "Boundary layer transition modeling on leading edge inflatable kite airfoils," *Wind Energy*, Vol. 22, 2019, pp. 908–921. https://doi.org/10.1002/we.2329.